

Document downloaded from:

<http://hdl.handle.net/10251/190351>

This paper must be cited as:

Martínez Fernández, P.; Villalba Sanchis, I.; Insa Franco, R.; Yepes, V. (2022). Slab Track Optimization Using Metamodels to Improve Rail Construction Sustainability. *Journal of Construction Engineering and Management*. 148(7):1-10.  
[https://doi.org/10.1061/\(ASCE\)CO.1943-7862.0002288](https://doi.org/10.1061/(ASCE)CO.1943-7862.0002288)



The final publication is available at

[https://doi.org/10.1061/\(ASCE\)CO.1943-7862.0002288](https://doi.org/10.1061/(ASCE)CO.1943-7862.0002288)

Copyright American Society of Civil Engineers

Additional Information

# 1 SLAB TRACK OPTIMISATION USING METAMODELS TO IMPROVE RAIL 2 CONSTRUCTION SUSTAINABILITY

3 Pablo Martínez Fernández<sup>a,\*</sup>, Ignacio Villalba Sanchís<sup>b</sup>, Ricardo Insa Franco<sup>c</sup>, Víctor Yepes<sup>d</sup>

## 4 **Abstract**

5 Railways are an efficient transport mode, but building and maintaining railways tracks  
6 has a significant environmental impact in terms of CO<sub>2</sub> emissions and use of raw  
7 materials. This is particularly true for slab tracks, which require large quantities of  
8 concrete. They are also more expensive to build than conventional ballasted tracks, but  
9 require less maintenance and have other advantages that make them a good alternative,  
10 especially for high-speed lines. In order to contribute to a more sustainable railways, this  
11 paper aims to optimise the design of one of the most common slab track typologies:  
12 RHEDA 2000. The main objective is to reduce the amount of concrete required to build  
13 the slab without compromising its performance and durability. To do so, a Finite Elements  
14 (FEM) model of the track has been used, paired with a kriging meta-model to allow  
15 analysing multiple options of slab thickness and concrete strength in a timely manner. By  
16 means of the kriging, optimal solutions have been obtained and them validate through the  
17 FEM model to ensure that predefined mechanical and geometrical constraints are met.  
18 Starting from an initial setup with a 30 cm slab made of concrete with a characteristic  
19 strength of 40 MPa, an optimised solution has been reached, consisting on a 24 cm slab

---

<sup>a</sup> PhD Civil Engineer. Department of Transport Engineering and Infrastructure. Universitat Politècnica de València (UPV). Camino de Vera, s/n, 46022, Valencia, Spain. Email: [pabmarfe@cam.upv.es](mailto:pabmarfe@cam.upv.es)

<sup>b</sup> PhD Civil Engineer. Department of Transport Engineering and Infrastructure. Universitat Politècnica de València (UPV). Camino de Vera, s/n, 46022, Valencia, Spain. Email: [igvilsan@cam.upv.es](mailto:igvilsan@cam.upv.es)

<sup>c</sup> PhD Civil Engineer. Department of Transport Engineering and Infrastructure. Universitat Politècnica de València (UPV). Camino de Vera, s/n, 46022, Valencia, Spain. Email: [rinsa@tra.upv.es](mailto:rinsa@tra.upv.es)

<sup>d</sup> PhD Civil Engineer. ICITECH. Universitat Politècnica de València (UPV). Camino de Vera, s/n, 46022, Valencia, Spain. Email: [vyepesp@cst.upv.es](mailto:vyepesp@cst.upv.es)

\*Corresponding author. Phone: +34 96 387 70 07 Ext. 73767

20 made of concrete with a strength of 45 MPa, which yields a cost reduction of 17.5%. This  
21 process may be now applied to other slab typologies to obtain more sustainable designs.

22 **Keywords:** Slab track; optimization; latin hypercube, kriging; finite elements

## 23 **1 Introduction**

24 Transport is one of the most essential human activities, and as such has a significant  
25 impact on Greenhouse Gasses (GHG) emissions. For instance, in the European Union,  
26 transport accounts for 24.6% of CO<sub>2</sub> equivalent emissions, the biggest share among all  
27 economic sectors except the energy sector (European Commission, 2020). Therefore,  
28 promoting a more sustainable transport and reducing its carbon footprint are crucial steps  
29 towards a cleaner society.

30 Railways are a rather efficient transport mode, as they contribute only 0.5% of the CO<sub>2</sub>  
31 equivalent emissions of the transport sector in the EU-27, despite carrying 6.9% of  
32 passengers and 12.4% of freight (European Commission, 2020). This explains the current  
33 trend of promoting railways across the EU as a way of reducing the environmental impact  
34 of transport (European Commission, 2018), which implies construction of new lines and  
35 renewal and maintenance of existing ones.

36 However, building and maintaining railway tracks have also a significant environmental  
37 impact in terms of GHG emissions and use of raw materials. For instance, according to  
38 Kortazar et al. (2021), the development of the Spanish High-Speed network requires up  
39 to 196.66 tonnes of CO<sub>2</sub> equivalent per year for construction and maintenance (compared  
40 to an estimated 355.68 tonnes of CO<sub>2</sub> equivalent per year for operation), considering the  
41 four main high-speed corridors. While studying the environmental impacts of the Beijing-  
42 Shanghai high-speed line, Kaewunruen et al. (2020) estimated that construction accounts  
43 for 64.86% of the total carbon emissions of the line (including operation and

44 maintenance), and that producing the cement required to build the slab track accounts for  
45 60% of the emissions due to construction.

46 These examples point out that constructing and maintaining railway tracks greatly  
47 contribute to the overall carbon footprint of this transport mode, to the extent that they  
48 may reduce (but not cancel) the reduction of GHG emissions that may be achieved by  
49 shifting to rail from other, less efficient modes (Åkerman, 2011). Therefore, optimising  
50 the track layout (and particularly, the amount of materials used to build the track) is of  
51 paramount importance to mitigate GHG emissions and to make railways an even better  
52 option for a more sustainable transport.

53 Although the conventional ballasted track remains the most common track layout across  
54 the world, ballastless (or slab) tracks are a rather interesting alternative, particularly for  
55 new high-speed lines. Slab tracks replace the ballast-and-sleeper package with a  
56 reinforced concrete slab (either made in situ or prefabricated). They are usually between  
57 1.5 and 2 times more expensive to build than ballasted tracks (Lichtberger, 2011).  
58 However, if properly built, require less maintenance than ballasted tracks over the years.  
59 Several studies have shown slab track maintenance costs to be up to 30% lower than those  
60 of ballasted tracks (Michas, 2012), which means that slab tracks are economically more  
61 efficient in the long term (Esveld, 2001; Michas, 2012). Additionally, slab tracks present  
62 other advantages such as longer life-cycle or better load distribution (Esveld, 2001;  
63 Michas, 2012), and may even be more sustainable in the long term, assuming service life  
64 over 75 years (Pons et al., 2020).

65 There are many different designs of slab tracks that have been used and tested over the  
66 last five decades. They may be roughly classified into two categories depending on  
67 whether the slab is prefabricated or cast in situ. Among the former are worth mentioning  
68 the Japanese Shinkansen slab, the German Bögl, the Austrian ÖBB-Porr or the Italian

69 IPA. Among the latter, the German RHEDA and Züblin or the French STEDEF (Gautier,  
70 2015; Michas, 2012). However, from an environmental point of view, all of them require  
71 large amounts of concrete (and thus cement) which, as pointed out previously  
72 (Kaewunruen et al., 2020), greatly contribute to their carbon footprint. To put this into  
73 context, a standard RHEDA 2000 layout (see Figure 1) requires approximately 1540 m<sup>3</sup>  
74 of reinforced concrete for the slab plus 2280 m<sup>3</sup> of mass concrete for the supporting layer  
75 per km of single track, hence a global figure of 3,82 m<sup>3</sup>/m. For comparison, the  
76 approximate amount of concrete used to build large rail bridges is 32 m<sup>3</sup>/m (Tuchschnid  
77 et al., 2011), but bridges are singular structures while tracks may cover hundreds of  
78 kilometres.

79 Therefore, optimising current slab designs to reduce their cost and environmental impact  
80 would have a noticeable effect on their sustainability. However, established slab designs  
81 have been carefully devised to offer long-term durability, resistance and reliability  
82 (Esveld, 2001), and thus optimising them taking into account environmental concerns is  
83 a complex task that should take into account several criteria.

84 In fact, in contrast to other areas of civil engineering, there has been little effort in recent  
85 years to optimise rail cross-sections and track typologies. Research has focused mostly  
86 on optimising vehicles, studying for instance their shape and aerodynamic performance  
87 (Jakubek and Wagner, 2016), wheel profiles or damping systems (Ye et al., 2021). A  
88 remarkable amount of work has also been devoted to eco-driving and energy efficiency  
89 (Eaton et al., 2017; Fernández et al., 2015; Martínez Fernández et al., 2019b).

90 However, optimisation of the rail infrastructure (and, particularly, the track) is a much  
91 less developed area of study, and has been applied basically to rail profiling and  
92 maintenance (Ye and Sun, 2021) or to reduce noise and vibration (Zhao et al., 2017).  
93 From an environmental point of view, other studies have focused on reusing waste

94 materials, particularly those produced in large quantities such as scrap tyres (Ferdous et  
95 al., 2021), to build track elements (Hidalgo Signes et al., 2016). Traditionally, rail track  
96 cross-section design has been based on experience and full-scale tests implemented by  
97 railway administrators. Thus, tracks are generally designed to meet operational and  
98 economical requirements, such as higher speeds or axle loads, with little regard paid to  
99 environmental concerns. A thorough optimisation of the track cross-section to reduce its  
100 carbon footprint, particularly for slab tracks, remains a task to be carried out within the  
101 railway sector.

102 In order to start filling this gap and contribute to a more sustainable railway, this paper  
103 aims to carry out an optimisation of the RHEDA 2000 slab design, one of the most  
104 common and tested slab tracks (Esveld, 2001; Michas, 2012). The main objective is to  
105 apply optimisation methods well tested in other areas of civil engineering to reduce the  
106 amount of concrete used to build the slab as well as its characteristic strength (and thus  
107 both its cost and GHG emissions) without compromising its performance and long-term  
108 durability. In this way, the paper pretends to test the applicability of said methods to  
109 optimise slab track cross-sections and to offer a first approach to an optimised RHEDA  
110 2000 slab track.

111 In order to do so, a Finite Element Model (FEM) of a ballastless railway track built with  
112 a RHEDA 2000 slab has been used. Although several approaches and methodologies are  
113 already available, the Finite Element Method (FEM) has proved to be a useful and  
114 effective tool for research on railway track elements (Esveld, 2001; Selig and Waters,  
115 1994; Zhao et al., 2017).

116 However, as calculating each and every alternative with the FEM model is unfeasible, a  
117 meta-model has also been used. Meta-models are simpler approximations to more  
118 complex models (such as the FEM in this case) which allow sifting out the solution space

119 in a timely manner and picking up optimal solutions (or rather, roughly optimal ones)  
120 than may be then checked with the FEM model.

121 There are many different meta-models and ways of creating them. Although many of  
122 them have been extensively compared in the past, deciding which one is better depends  
123 on the specific problem to be solved. That said, there are certain models that are more  
124 commonly used, such as polynomial regression, neural networks (García-Segura et al.,  
125 2018; Martínez Fernández et al., 2019a) or kriging (Penadés-Plà et al., 2020b). In this  
126 paper, kriging has been chosen as it is more flexible than polynomials and is less time-  
127 consuming than neural networks (Simpson et al., 2001). Moreover, it is already been used  
128 for structural optimisation in other areas of civil engineering such as bridge construction  
129 (Penadés-Plà et al., 2020a), or even in railways to optimise wheel profiles and train  
130 suspension (Ye et al., 2021).

131 The paper is organised as follows: first, a detailed description of the optimisation problem  
132 is given, and the FEM model, the meta-model (kriging) and other tools used are explained.  
133 Then, the results obtained from the optimisation process are given and discussed, and  
134 finally the main conclusions achieved are explained, together with insights for further  
135 research.

## 136 **2 Materials and methods**

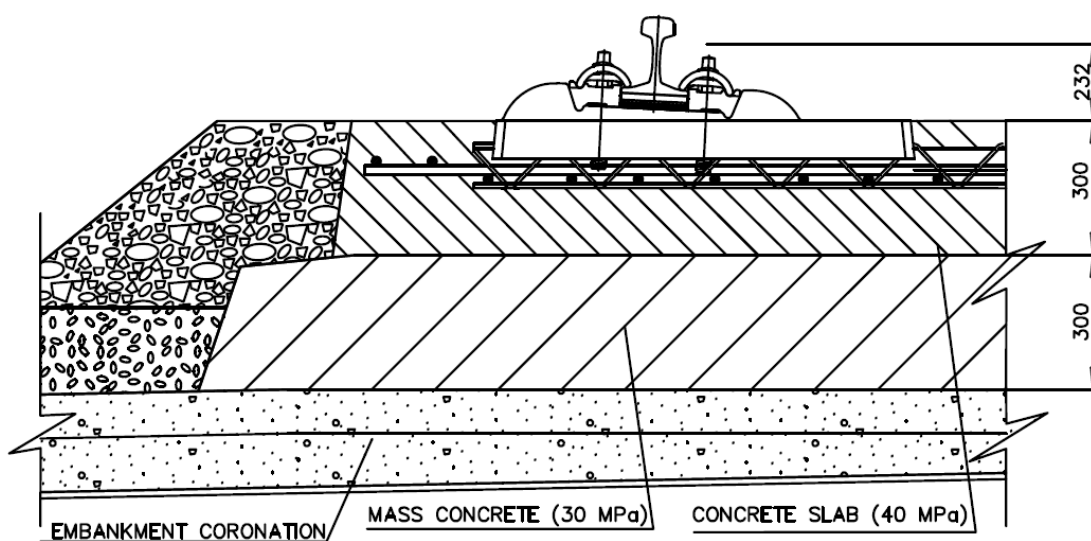
### 137 **2.1 Optimisation problem description**

138 As explained before, the main objective of this paper is to carry out an optimisation of an  
139 existing slab track design (RHEDA 2000), seeking to reduce its costs and environmental  
140 impact without compromising its performance and durability. The RHEDA 2000 is, as  
141 stated before, one of the most common slab track typologies, but the optimisation process  
142 presented in this paper could be applied to other slab tracks such as Shinkansen, Bögl,

143 Züblin or Stedef, as they all are based on a monolithic concrete slab (be it prefabricated  
144 or built in situ) that replaces the ballast layer (Michas, 2012).

145 The RHEDA 2000 is a slab track system with discrete rail support: the continuous rail is  
146 fastened to concrete sleepers which are, in turn, embedded in a monolithic concrete slab  
147 (Michas, 2012). The original RHEDA system was first used in 1972 in Germany, and has  
148 been updated and improved over the years. The current RHEDA 2000 version was first  
149 used for parts of the high-speed line between Leipzig and Halle (Esveld, 2001), and has  
150 since become one of the most used slab systems in the world (Michas, 2012).

151 In this study, a standard RHEDA 2000 layout has been considered (figure 1). The slab  
152 has a thickness of 30 cm and is made of concrete with a characteristic strength of 40 MPa.  
153 The slab rests over a layer (thickness: 30 cm) of mass concrete (strength: 20 MPa) and an  
154 embankment coronation layer (thickness: 30 cm) of soil cement. The rails are UIC60 and  
155 the fastening system consists on IOARV 300 fasteners with Vossloh clips (model SKL  
156 15). It would be interesting to also analyse the economic and environmental impact of  
157 track fastening elements, but this is a complex task in itself and beyond the scope of this  
158 paper.



159  
160

**Fig 1.** RHEDA 2000 half cross-section with initial design variables. Distances in mm.



161 The main assumption on which the optimisation process will be based is that reducing the  
162 cost of the track section (and, specifically, of the slab) will in turn yield a drop of its  
163 environmental impact and an improvement of its sustainability (owing to the reduction of  
164 raw materials used). This is justified by the large quantities of concrete required to build  
165 a single km of RHEDA 2000 (roughly 1540 m<sup>3</sup>/km only for the slab, considering the  
166 layout shown in Figure 1), and the significant impact that concrete and cement production  
167 have on the environment (Mohamad et al., 2021).

168 Therefore, our objective function is expressed as:

$$169 \min\{C(e, f_{ck}) = \frac{e}{100} \cdot 2.6 \cdot 1000 \cdot P(f_{ck}) = 26 \cdot e \cdot P(f_{ck})\} \quad (1)$$

170 Where  $C(e, f_{ck})$  is the total cost in € of 1 km of slab track,  $e$  is the slab thickness in cm,  $f_{ck}$   
171 is the characteristic strength in MPa of the concrete used to build the slab and  $P(f_{ck})$  is the  
172 unitary cost in €/m<sup>3</sup> of said concrete. The reason for choosing these two variables is that  
173 slab thickness is the only slab dimension that may be modified to achieve a substantial  
174 reduction of the amount of concrete used (as slab width is constrained by track geometric  
175 requirements). Moreover, a thinner slab may require a stronger concrete to resist traffic  
176 loads, which increases costs and also implies higher quantities of cement. Therefore, these  
177 two variables not only have a direct impact on slab cost, but are also correlated to each  
178 other.

179 That said, the objective is to minimise Equation (1), which means dealing with those two  
180 design variables: slab thickness ( $e$ ) and concrete characteristic strength ( $f_{ck}$ ). Considering  
181 usual concrete characteristics as per Eurocode 2 (CEN, 2004) and usual geometric  
182 requirements for the slab based on RHEDA 2000 tracks in service (Cortina Ruiz, 2013;  
183 Michas, 2012), these two variables will be within the following ranges:

$$184 \begin{cases} e \in [10,40]cm \\ f_{ck} \in [30,45]MPa \end{cases} \quad (2)$$

185 Where  $e$  will be varied in intervals of 1 cm and  $f_{ck}$  in intervals of 5 MPa. Of course, as  
186 explained before, there are several criteria to be considered to ensure that any combination  
187 of  $e$  and  $f_{ck}$  values within the ranges of Equation (2) that minimise Equation (1) yield a  
188 resistant and durable slab. In order to set up such criteria, several Spanish and  
189 international standards for railway construction have been considered, including Spanish  
190 Recommendations for Railway Infrastructures (Ministerio de Fomento, 1999) and ADIF  
191 Standards (ADIF, 2000), as well as UIC 719R (UIC, 2008). From these regulations and  
192 recommendations, the following requirements have been defined:

- 193 • Maximum vertical displacement in rail:  $\delta_y \leq 3\text{mm}$ .
- 194 • Maximum stress in rail (Von Mises criterion):  $\sigma_{vm} \leq 137.5\text{ MPa}$
- 195 • Vertical track stiffness (based on (Pita et al., 2004)):  $k \in [75,85]\text{ kN/mm}$
- 196 • Maximum traction stress in slab:  $\sigma_{adm} \leq f_{tck}/4.1$  (where  $f_{tck}$  is the concrete  
197 characteristic tensile strength).

198 Therefore, any optimal solution obtained during the process should comply with all these  
199 constraints to ensure that the resultant slab does not compromise track performance.

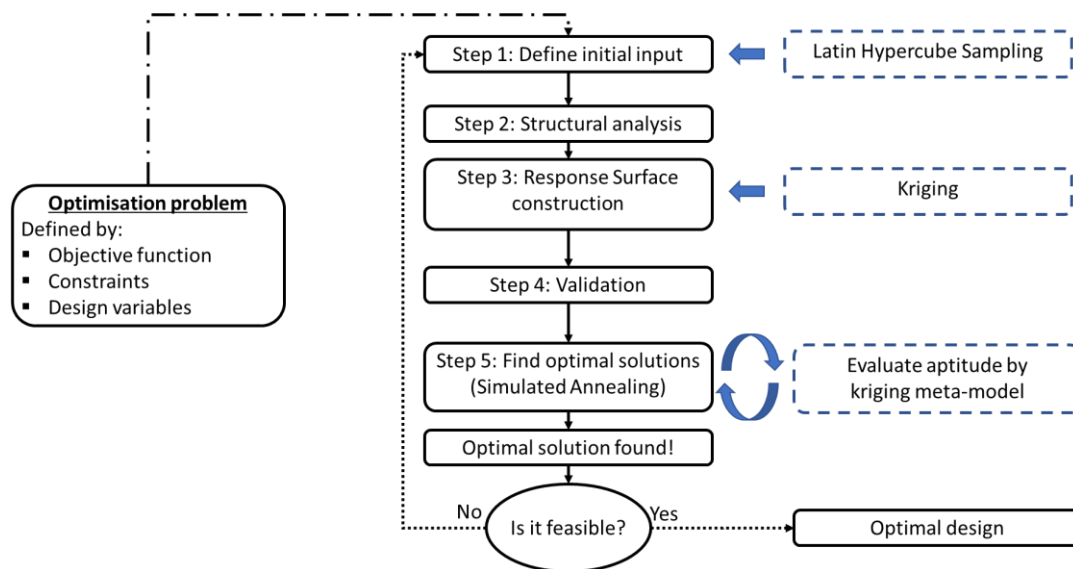
200 In order to assess the different combinations of slab thickness and concrete strength and  
201 calculate the track performance (and all the aforementioned displacements and stresses),  
202 a FEM model of the track was used. FEM models have been extensively used to model  
203 track dynamics (Connolly et al., 2013; Martínez Fernández et al., 2013; Villalba Sanchis  
204 et al., 2021) and are thus a reliable tool to analyse the behaviour of any variation of the  
205 RHEDA system. However, FEM models are also time-consuming because, in order to  
206 properly model the track section (and considering that a sufficient length of track must be  
207 modelled to avoid boundary disturbances), they usually consist on hundreds of thousands  
208 of elements (Hall, 2003; Sayeed and Shahin, 2016) even accounting for symmetry  
209 simplifications (which are not always possible). Considering also moving, dynamic loads

210 (to simulate the passing of a train), FEM simulations require indeed high computational  
211 costs and running time, although the exact figure depends on model complexity and  
212 computer assets available (Jin et al., 2018; Li et al., 2018). Therefore, it is not feasible to  
213 directly use a FEM model to test all the possible combinations of  $e$  and  $f_{ck}$  within the  
214 ranges shown in Equation (2). Consequently, a meta-model was used instead to carry out  
215 the bulk of the optimisation process, leaving the FEM model as a validation check for the  
216 few, best solutions obtained via the meta-model. As explained before, meta-models are  
217 simpler approximations to more complex models (in this case, the FEM model of the  
218 track) which provided a rough and fast estimation of the results that the main model would  
219 yield for a given input. This is expressed in Equation (3):

$$220 \quad y = f(x) = g(x) + \varepsilon \quad (3)$$

221 Where  $x$  are the input variables for the model,  $f(x)$  is the output of the main model,  $g(x)$   
222 is the output of the meta-model and  $\varepsilon$  is the meta-model error. There are several  
223 mathematical approaches to define and create the metamodel  $g(x)$ , but in this case the  
224 kriging model was used because it has lower computational requirements than other  
225 similar approaches (Simpson et al., 2001) and thus provides solutions faster (which is, as  
226 explained before, one of the reasons for using meta-models instead of the FEM full  
227 model). Another advantage is that kriging is more flexible due to its formulation, but this  
228 is further explained in section 2.3.

229 Figure 2 shows a flow chart of the optimisation process, whose different steps and  
230 elements are explained in more detail in the following subsections.



231

232 **Fig. 2.** Flow chart of the optimisation process. Adapted from Penadés-Plà et al. (2019).

## 233 2.2 Input selection

234 As shown in Figure 2, once the optimisation problem is defined (with objective function,  
 235 design variables and constraints), the first step of the process is to obtain an initial  
 236 population that will be then used to build the meta-model. How this input set is obtained  
 237 will have a crucial impact on the meta-model accuracy, as it must be representative of the  
 238 solution space (i.e. the space defined by all the possible values of each input variable).

239 The input set is defined by its size and location across the solution space. Input size is  
 240 directly related to the number of variables, which in our case amounts to two (namely,  
 241 slab thickness  $e$ , and concrete characteristic strength  $f_{ck}$ ). As for how to sample each  
 242 variable across its respective range to obtain the most representative input set, a form of  
 243 Design of Experiments (DOE) should be used.

244 There are many different techniques that belong to the DOE approach, from classical  
 245 methods (such as Box-Behnken or D-optimal (Myers et al., 2016)) to space filling  
 246 methods, more apt for complex meta-models as they cover the whole solution space to  
 247 account for local phenomena. Among the latter, the most common is the Latin Hypercube  
 248 (Dette and Pepelyshev, 2010). This is the one chosen in this paper, as it has been used in

249 previous studies of structural optimisation (Penadés-Plà et al., 2020b, 2019) and it is  
250 comparatively more efficient (i.e. provides samples faster) than other common sampling  
251 techniques (Olsson et al., 2003; Woods and Lewis, 2017).

252 The Latin Hypercube determines a number  $n$  of non-overlapping intervals for each  
253 variable  $v$  and number of input points  $n$ . This divides the solution space into  $n \times v$  regions  
254 so that each initial input point is placed in one region, thus ensuring that all variables are  
255 sampled across their whole range.

256 The population sampled through the Latin Hypercube is then analysed to obtain not only  
257 the value of the objective function (Equation 1) but also the corresponding values for each  
258 of the predefined constraints. The latter is done by means of the FEM model described in  
259 section 2.5.

### 260 **2.3 Kriging meta-model**

261 With the input sampled using the Latin Hypercube as described above, it is possible to  
262 generate the meta-model. As explained before, the one chosen for this study is the kriging  
263 model, which was first proposed by Danie Kirge for geo-statistical applications and later  
264 formalised by Matheron (Matheron, 1963). The kriging meta-model is formulated  
265 according to Equation (4):

$$266 \quad y(x) = f(x) + Z(x) \quad (4)$$

267 Where  $y(x)$  is the deterministic output to be obtained,  $f(x)$  is a defined approximation  
268 function (similar to a regression model) and  $Z(x)$  is a stochastic process with mean  $\mu = 0$   
269 and variance  $\sigma^2 \neq 0$ . The purpose of the stochastic addition is to generate local variations  
270 for the kriging to interpolate between the initial input data.

271 There are different versions of the kriging approach formulated in Equation (4). The most  
272 common (i.e. ordinary kriging) uses a constant  $f(x)$  term. Furthermore, if  $f(x)$  tends to zero

273 (which means that  $y(x)$  as a mean value close to zero too), the model is known as simple  
274 kriging (Simpson et al., 2001).

275 Regarding the precise formulation of  $f(x)$ , the most common form (and the one used in  
276 this paper) is that of a weighted linear combination as shown in Equation (5):

$$277 \quad f(x) = \sum_{i=1}^n \beta_i \cdot f_i(x) \quad (5)$$

278 Where  $f_i(x)$  are already known outputs (that is, the dataset used to build the meta-model)  
279 and  $\beta_i$  are the corresponding weights (Biles et al., 2007). As for the stochastic term  $Z(x)$   
280 of Equation (4), its usually defined as follows:

$$281 \quad \begin{cases} cov[Z(x_i), Z(x_j)] = \sigma^2 \cdot R(x_i, x_j) \\ R(x_i, x_j) = e^{-\sum_{k=1}^m \theta |x_k^i - x_k^j|^2} \end{cases} \quad (6)$$

282 Note that  $\sigma^2$  scales the spatial correlation function  $R(x_i, x_j)$ , which in turn is usually  
283 (Simpson et al., 2001) expressed as a gaussian correlation function with a single  
284 parameter  $\theta$ . A lower value of  $\theta$  means that all the points in the sample are highly  
285 correlated and thus the  $Z(x)$  term in Equation (4) remains similar in the whole solution  
286 space. On the other hand, as the  $\theta$  value increases, the more correlated points are closer  
287 and the  $Z(x)$  term will vary across the solution space. This allows for a more flexible  
288 approach than other similar meta-models which do not allow tuning the spatial correlation  
289 (Simpson et al., 2001).

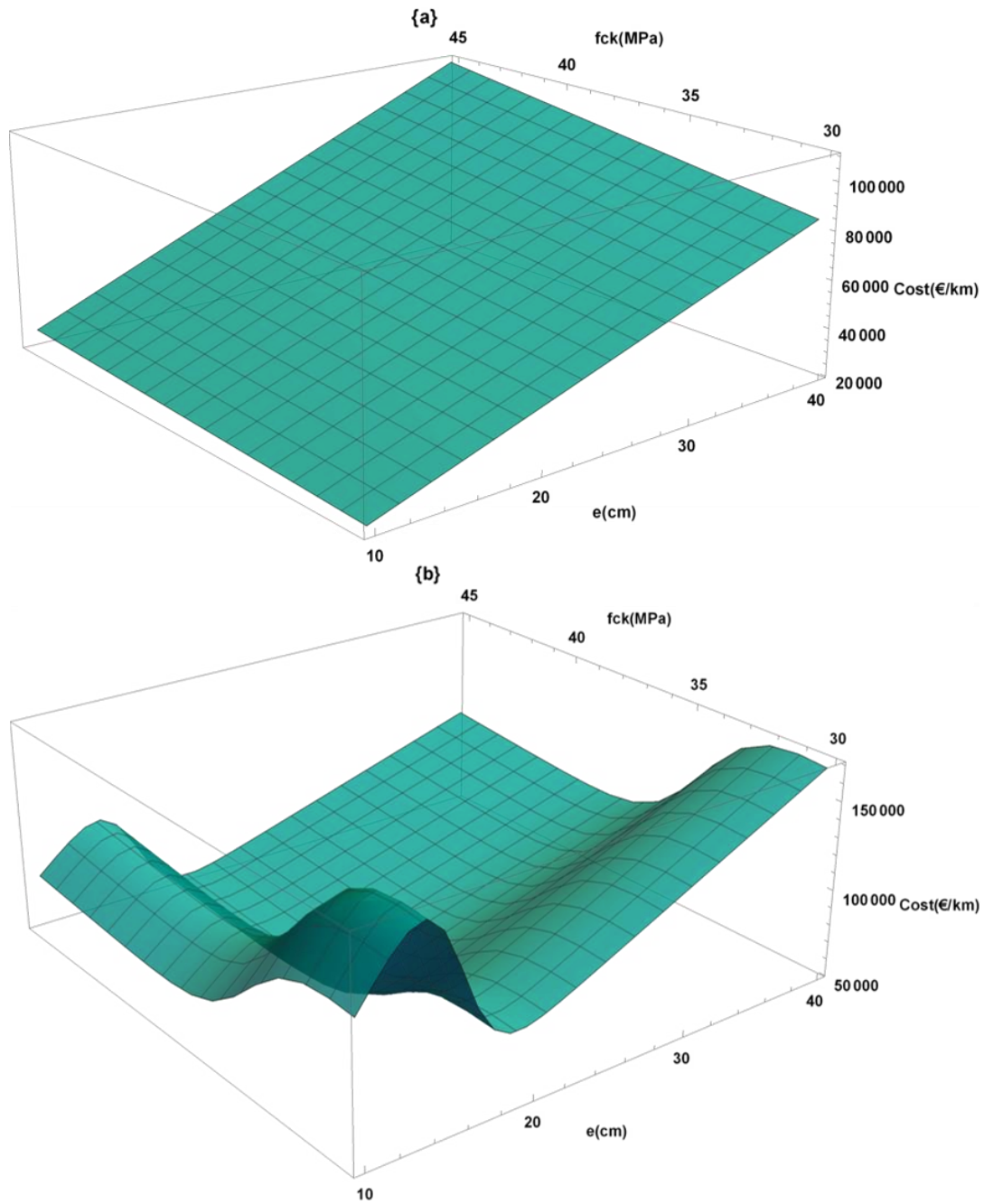
290 Finally, the kriging model requires an associated method to fit the initial input data, which  
291 in this case, based on previous research (Penadés-Plà et al., 2019), is the Best Linear  
292 Unbiased Prediction method (BLUP).

## 293 **2.4 Optimisation process, surfaces**

294 In order to solve the optimisation problem defined in section 2.1 by means of the kriging  
295 meta-model, the process summarised in Figure 2 is followed. Therefore, once the initial  
296 output set has been sampled using the Latin Hypercube, the meta-model described in

297 section 2.3 may be used to generated a response surface, which is an estimation of the  
298 output of Equation 1 by the meta-model.

299 However, as Equation 1 only calculates the cost of the slab considering two design  
300 variables (thickness  $e$ , and concrete strength  $f_{ck}$ ), the response surface will take the form  
301 shown in figure 3a. Of course, in that case the cheaper solution will be that with the  
302 shallower slab ( $e = 10$  cm) and weakest concrete ( $f_{ck} = 30$  MPa), but this slab layout might  
303 not ensure a proper performance. In order to take into account the constraints defined in  
304 section 2.1, penalties are applied to the response surface in the form of a coefficient that  
305 multiplies the value of the objective function (in this case, the cost of the slab). This  
306 coefficient is defined as the quotient between the exceeding value and the admissible  
307 value for each constraint, raised to the power of 5 (as usually this quotient is only slightly  
308 over 1, and without raising it to a high power, it would barely affect the outcome). By  
309 applying this coefficient to the kriging output, the response surface is altered, taking a  
310 shape similar to that in figure 3b.



311

312 **Fig. 3.** Response surface obtained with kriging. (a) Surface without constraints. (b)

313 Surface with constraints applied through penalties.

314 This is now a complex surface with local maxima (solutions that do not comply with  
 315 constraints) and minima (solutions that do comply all constraints). The surface may take  
 316 different shapes depending on the input dataset used to build the meta-model and may  
 317 present many local minima. Therefore, identifying the global minimum (which would  
 318 yield an optimal slab layout) is done by means of a meta-heuristic algorithm. The one



319 used in this work is Simulated Annealing (SA) as it is a versatile algorithm capable of  
320 finding global optimums (Kirkpatrick et al., 1983).

321 SA is an algorithm inspired by the annealing process in metallurgy. It is an iterative  
322 process where the current state of the objective function (in this case, the cost of the slab)  
323 is compared to nearby states in the response surface, looking for lower values. A detailed  
324 description of the algorithm may be found in Ghasemalizadeh et al. (2016) and  
325 Kirkpatrick et al. (1983). Regarding the SA parameters, they have been calibrated  
326 following the process found in Medina (2001) to define the initial temperature, adopting  
327 a cooling coefficient ( $k$ ) of 0.8.

328 Of course, introducing those penalties to account for mechanical and geometrical  
329 constraints causes uncertainty to the cost estimation done by the kriging meta-model. To  
330 address this issue, up to nine response surfaces have been generated, each one based on a  
331 different sampling of initial pairs of  $e$  and  $f_{ck}$  obtained with the Latin Hypercube. This  
332 will, in turn, yield nine optimal solutions for our optimisation problem that can be then  
333 analysed in more detail and validated using the whole model i.e. the FEM track model.

334 The kriging model creation, the generation of response surfaces and the calculation of  
335 optimal solutions by means of a heuristic algorithm were all carried out using *MATLAB*  
336 2018a (The Mathworks, Inc.) with the DACE toolbox developed by Lophaven et al.  
337 (2002).

## 338 **2.5 Validation with FEM**

339 As explained before, FEM models have been extensively used to model the mechanical  
340 behaviour of the track (Esveld, 2001; Selig and Waters, 1994; Zhao et al., 2017). These  
341 models can simulate the tensional and deformation state by discretizing the track structure  
342 to finite elements and solving the resulting mathematical equations. Thus, the track  
343 superstructure and substructure, subjected to specific boundary conditions and

344 restrictions, may be analysed as a whole, considering interactions between all  
345 components.

346 In the context of this study, the FEM model represents the most accurate simulation of  
347 the track behaviour, and it is used in two stages: First, to evaluate the constraints of the  
348 initial datasets sampled by the Latin Hypercube and used to generate the kriging meta-  
349 model, and secondly, to validate the optimal solutions provided by identifying the global  
350 minimum of each response surface generated by the kriging. The latter is required because  
351 the meta-model, as an approximation of the FEM model, provides optimal solutions in a  
352 timely manner but, in doing so, assumes a higher degree of uncertainty. The FEM model,  
353 which provides more accurate values of stress and strain in every element of the track,  
354 helps checking that the optimal solutions provided by the kriging meta-model do fulfil all  
355 the technical constraints defined in section 2.1.

356 The RHEDA 2000 slab track is modelled as a parametrized three-dimensional track,  
357 where rails are discretely supported above each sleeper, which in turn are directly  
358 embedded in the concrete, forming a monolithic slab (Figure 4). Rails are modelled as a  
359 uniaxial three-dimensional solid element with twenty nodes with tensile, compression,  
360 bending and torsion behaviour. The rail pad is represented by a spring-damper element  
361 with two nodes that behaves in uniaxial tension-compression. In addition, the sleepers  
362 and the multilayer system use a three-dimensional solid element with three degrees of  
363 freedom per node: translations in X, Y and Z. Conventional values of stiffness and  
364 strength are used for concrete and steel elements. Finally, the values given by the UIC  
365 soil classification are used as a reference for the embankment.

366 The model has a total length of 5.4 metres, covering 9 sleepers with a separation of 0.6  
367 m. The slab width is 2.6 m (equivalent to a single track with standard gauge). However,  
368 as the track is completely symmetrical along the longitudinal axis, only half track is

369 modelled. Regarding the loads, a high-speed TALGO 102 series is considered with a  
370 static axle load of 167 kN (and hence a wheel load of 83.5 kN). However, in order to  
371 account for dynamic effects, this static load is raised using the Eisenmann criterion,  
372 yielding a total wheel load of 116.9 kN (considering a train speed of 300 km/h).  
373 The FEM model was created and run in *ANSYS Mechanical APDL 17.2* (Ansys, Inc.).

### 374 **3 Results and discussion**

#### 375 **3.1 Surfaces obtained and table of optimal results for each one.**

376 The whole optimisation process described in Figure 2 has been applied to obtain optimal  
377 combinations of slab thickness ( $e$ ) and concrete characteristic strength ( $f_{ck}$ ) than minimise  
378 cost (Equation 1) while complying with all the constraints described in section 2.1.

379 In order to ensure that the whole solution space is analysed, the Latin Hypercube method  
380 was applied nine times to obtain nine different input sets, which in turn were used to build  
381 nine meta-models and obtain the same number of surfaces from which the heuristic  
382 algorithm could get an optimal solution. The results are shown in Table 1.

383 The first noteworthy result is that every optimal solution obtained from each of the nine  
384 surfaces generated through kriging complies with the four main constraints, and thus all  
385 of them are feasible solutions that do not compromise the slab performance. This justifies  
386 the use of penalties to modify the response surfaces and avoid optimal solutions that are  
387 not constraint-compliant.

388 In terms of cost (the parameter to be minimised), Table 2 shows the cost value for each  
389 optimal solution as given by the kriging model, and the comparison with the real cost  
390 calculated directly from Equation 1. There is an evident discrepancy between real and  
391 predicted costs due to the penalties introduced to the surfaces as explained in section 2.4.

392 This points out that using the meta-model implies a certain degree of error (as expressed

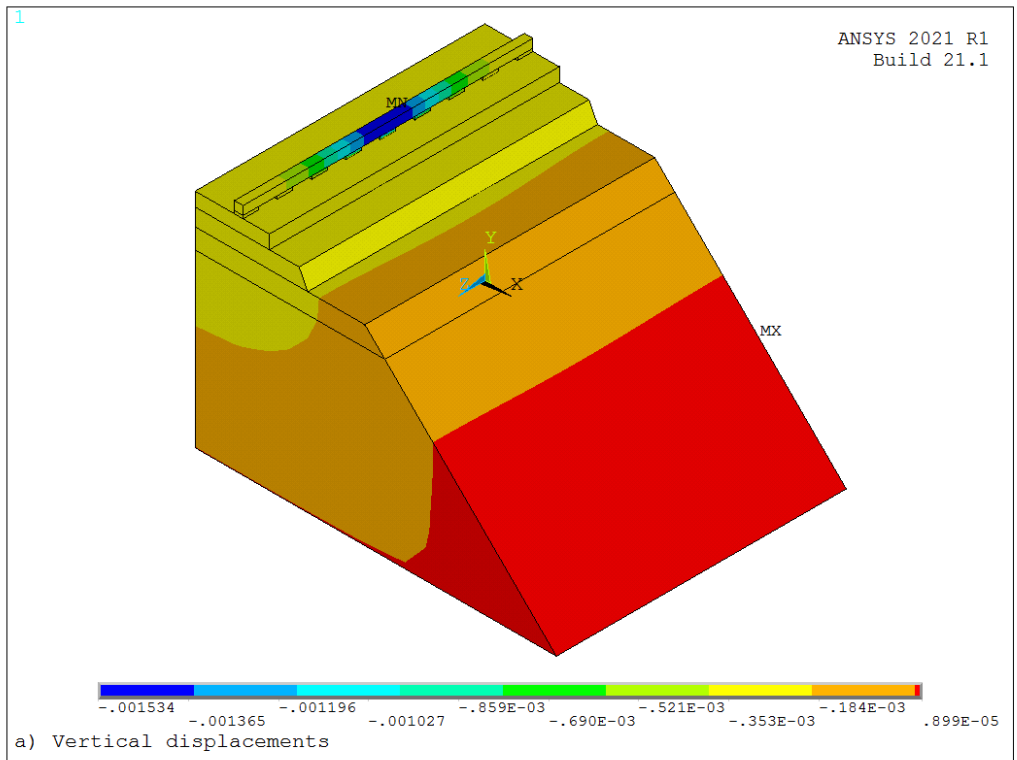
393 in Equation 3), but as the mean error is below 4.35% it is deemed acceptable for our  
394 purposes.

395 In any case, according to the results of Table 2, the solution which provides the greater  
396 cost reduction of the slab when compared to the original setup (i.e. a slab thickness of 30  
397 cm and a concrete strength of 40 MPa) is the one obtained from the ninth surface ( $e = 24$   
398 cm and  $f_{ck} = 45$  MPa). This solution yields a 17.15% cost reduction. Note that the same  
399 optimised setup was also obtained from the sixth surface, only in this case the estimation  
400 of cost given by the meta-model was higher.

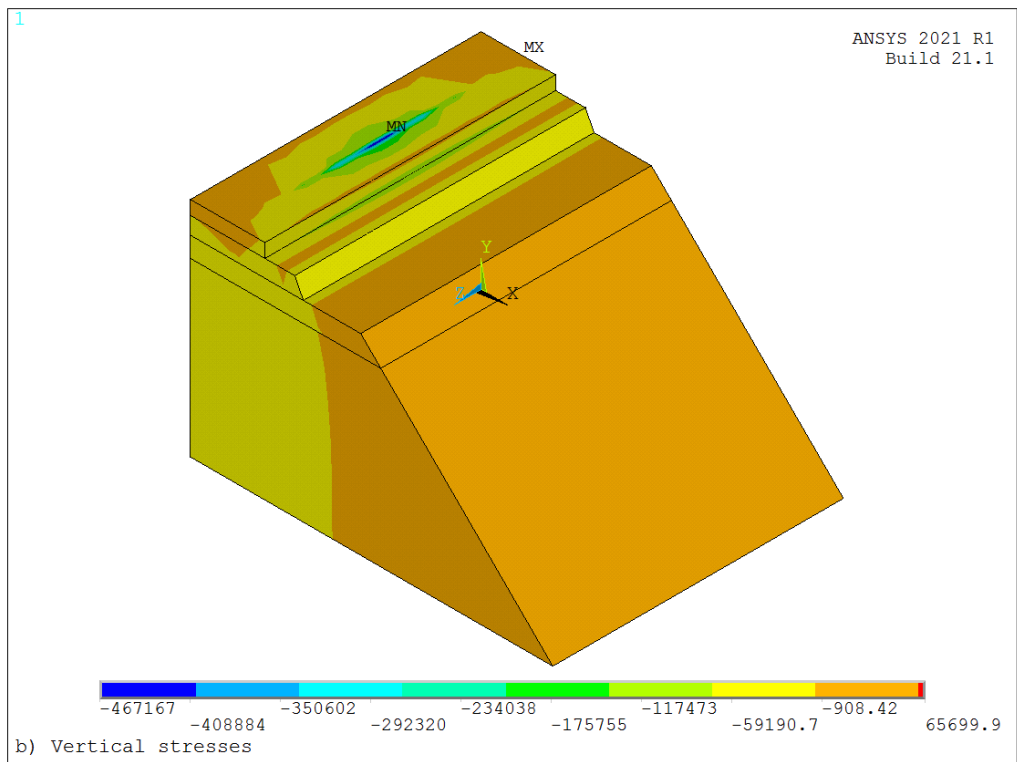
401 It is also worth noting that the optimal solution from the 8<sup>th</sup> surface yields a cost variability  
402 of 0 (which means that the cost figure given by the meta-model is equal to the real cost).  
403 This is due to the fact that, in that case, the optimal value belonged to the initial set  
404 sampled by the Latin Hypercube and used to build the meta-model.

### 405 **3.2 Validation with FEM**

406 In order to validate the optimal setup obtained (i.e.,  $e = 24$  cm and  $f_{ck} = 45$  MPa), the  
407 complete FEM model was used to check all constraints with more detail and accuracy.  
408 Only the slab thickness and concrete characteristic strength are modified to represent the  
409 optimal solution, with all other geometric and mechanic parameters of the FEM model  
410 fixed as defined in section 2.5. Figure 5 shows an excerpt of the main results yielded by  
411 the model in terms of vertical displacements (5a) and stresses (5b).



412



413

414

**Fig. 4.** FEM model results. a) Vertical displacements. b) Vertical stresses.

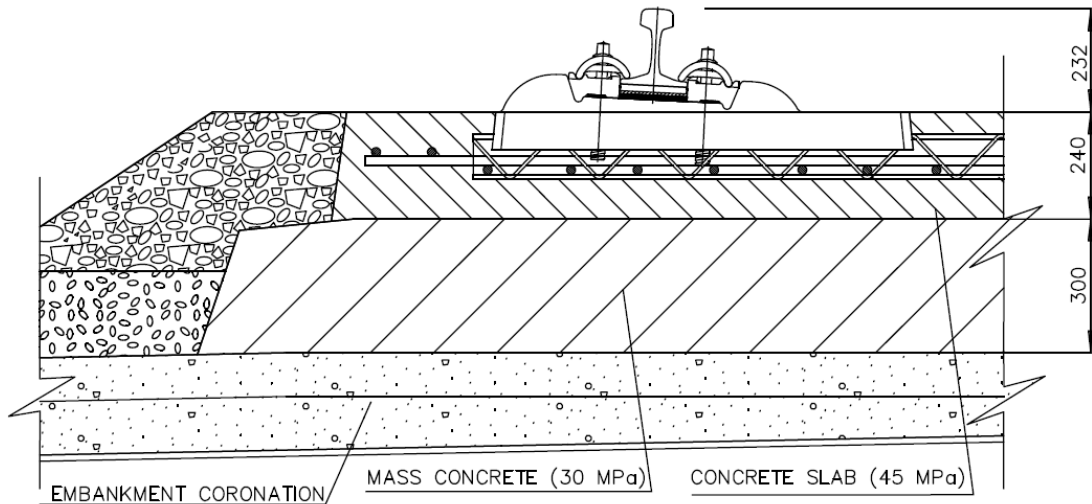
415

416

417

According to the FEM model, by using a slab with a thickness of 24 cm, made of a concrete with a characteristic strength of 45 MPa, the resultant track complies with all the predefined constraints. Specifically, the vertical displacement in the rail is 1.5 mm, thus

418 below the threshold value of 3 mm. Moreover, the overall track vertical stiffness is 78  
 419 kN/mm (well within the range of [75,85]) and the maximum stress is below the predefined  
 420 threshold for every material (i.e. rail, slab, platform). Therefore, the optimal setup  
 421 obtained using the kriging meta-model is a feasible solution that ensures a correct slab  
 422 performance. Figure 6 shows a track cross-section with the optimised variables.



423  
 424 **Fig. 5.** Track half cross-section with optimised variables. Distances in mm.

425 Finally, to further assess the potential advantages of the optimal solution, compared to  
 426 the original setup, a life-cycle analysis has been carried out. This analysis is based on the  
 427 *ReCiPe* methodology proposed by Goedkoop et al. (2009), with data from the  
 428 *ECOINVENT* database (Frischknecht and Rebitzer, 2005), and was carried out using  
 429 *OpenLCA* open source software. The *ReCiPe* method combines both midpoint and  
 430 endpoint indicators, but in this study only the latter have been considered as they provide  
 431 a more global and easier to compare assessment. These indicators consist on four  
 432 categories that evaluate the impact of each alternative studied by grouping many different  
 433 specific parameters:

- 434 • Impact in resources, measured in US dollars.
- 435 • Impact on ecosystems, measured in lost species per year.
- 436 • Impact on human health, measured in disability-adjusted life years.

437       • Impact on safety, measured in hours of average risk.

438 This methodology has already been used by other authors to perform life cycle  
439 assessments in civil engineering (Ata-Ali et al., 2021; Pons et al., 2018). The results are  
440 shown in Table 3.

441 As the table shows, the optimised cross-section not only reduces costs by 17.2%, but also  
442 yields a 15.27% reduction in the use of resources and a 37.50% reduction in the impact  
443 to ecosystems. Moreover, the new solution also improves health and safety.

444 Overall, the results obtained prove that the chosen methodology, based on a FEM model  
445 and a kriging meta-model, may be applied to track optimisation. This contributes to start  
446 filling the gap previously identified, namely the lack of thorough optimisation studies of  
447 track cross-sections (particularly slab designs) that consider environmental concerns. By  
448 using an optimisation methodology similar to the one proposed in this paper, which has  
449 already been tested in other areas of civil engineering, it is possible to obtain refined slab  
450 designs with reduced costs and use of materials. In this way, well-established slab  
451 typologies such as the RHEDA 2000 analysed in this paper could be modified to reduce  
452 their environmental impact and help improving the overall sustainability of railways,  
453 particularly with regard to their construction and maintenance.

454 Of course, the optimised RHEDA 2000 achieved in this paper is but a first approach to a  
455 complex matter, and further studies should be carried out to incorporate other factors into  
456 the analysis and to account for elements such as track subgrade or fastening systems,  
457 which have been omitted. Another noteworthy line of research would be to consider  
458 recycled aggregates or concrete for the construction of the slab, as using such materials  
459 may reduce the environmental impact of the infrastructure (Wang et al., 2021).  
460 Nevertheless, this approach paves the way for further optimisation in railways  
461 construction and sustainability, as it provides a fast and useful tool for railway engineers

462 to introduce environmental concerns into rail track design without requiring complex and  
463 time-consuming FEM models. Moreover, as slab tracks are becoming a noteworthy  
464 choice for new high-speed lines in many countries, the methodology presented in this  
465 paper may help achieving more optimised designs which will reduce the carbon footprint  
466 of rail construction and will help making railways an even more sustainable transport  
467 mode.

## 468 **4 Conclusions**

469 This paper aims to apply an optimisation methodology based on a FEM model and a  
470 kriging meta-model to offer a new approach into the reduction of the environmental  
471 impact linked to track construction. This methodology is tested with one of the most used  
472 slab track designs: RHEDA 2000. This is a monolithic slab track with discrete supports  
473 that has been extensively built for high-speed lines in countries such as Germany.  
474 Building a slab track implies a remarkable environmental impact in terms of raw materials  
475 (particularly, cement), which reduces to some extent the environmental benefits of  
476 building new railway tracks to shift passengers and freight to rail from other, less  
477 sustainable transport means.

478 In order to reduce the carbon footprint of the RHEDA 2000 slab track, the slab design has  
479 been optimised, trying to minimise its costs as an indirect way of alleviating the amount  
480 of concrete used as well as its characteristic strength (which in turn reduces the amount  
481 of cement). The methodology used to do so consists on a FEM model of a railway track  
482 with a RHEDA 2000 slab, created to test different slab designs with varying slab thickness  
483 ( $e$ ) and concrete characteristic strength ( $f_{ck}$ ). However, as FEM models are time-  
484 consuming, a meta-model has been used instead to analyse the whole solution space,  
485 saving the FEM model only for final validation.



486 Using a kriging meta-model, built upon nine different initial datasets (all sampled using  
487 a Latin Hypercube method), nine response surfaces have been created. Each one yielded  
488 an optimal solution (obtained by means of Simulated Annealing), that is, a pair of values  
489  $e$  and  $f_{ck}$  that minimise slab cost while also complying with certain, predefined mechanical  
490 and geometrical constraints. These constraints were applied to ensure that any optimal  
491 solution found does not compromise the track performance.

492 The best of the nine solutions obtained has a thickness of 24 cm and is made of concrete  
493 with a characteristic strength of 45 MPa. Its cost is 52,965.12 €/km, which represents a  
494 17.15% reduction when compared to the original setup ( $e = 30$  cm,  $f_{ck} = 40$  MPa). This  
495 slab setup has been then validated using the FEM model, and complies with all the  
496 predefined constraints. In order to further assess its environmental benefits, a life-cycle  
497 assessment has been carried out. According to this analysis, the optimised slab setup  
498 yields a 15.27% reduction in the use of resources and a 37.50% reduction in the impact  
499 to ecosystems, among other benefits.

500 This work aims to offer a first approach to slab track optimisation, filling a clear gap in  
501 the literature with regard to rail infrastructure optimisation. The proposed approach uses  
502 meta-models (i.e. kriging) as a useful methodology that does not required the amount of  
503 time and computing resources that whole track models (mainly based on FEM) would  
504 require. Although an optimised setup for a well-known and used slab design (RHEDA  
505 2000) has been achieved, the study could be further extended to other track typologies  
506 (both ballasted and ballastless), and improved by including other factors and criteria in  
507 the optimisation process.

508 **Data availability statement**

509 Some or all data, models, or code that support the findings of this study are available from  
510 the corresponding author upon reasonable request. (Kriging code in MATLAB, FEM  
511 model in ANSYS.)

## 512 **Acknowledgements**

513 The authors wish to thank Joaquin J. Pons for his work, which has been extremely helpful  
514 in the development of this paper. Grant PID2020-117056RB-I00 funded by MCIN/AEI/  
515 10.13039/501100011033 and by “ERDF A way of making Europe”. Funding for open  
516 access charge: CRUE-Universitat Politècnica de València.

## 517 **References**

- 518 ADIF, 2000. Sistemas de vía sobre base de hormigón y tacos prefabricados [WWW  
519 Document]. URL <http://descargas.adif.es/ade/u18/GCN/NormativaTecnica.nsf>  
520 (accessed 7.28.21).
- 521 Åkerman, J., 2011. The role of high-speed rail in mitigating climate change - The  
522 Swedish case Europabanan from a life cycle perspective. *Transp. Res. Part D*  
523 *Transp. Environ.* 16, 208–217. <https://doi.org/10.1016/j.trd.2010.12.004>
- 524 Ata-Ali, N., Penadés-Plà, V., Martínez-Muñoz, D., Yepes, V., 2021. Recycled versus  
525 non-recycled insulation alternatives: LCA analysis for different climatic conditions  
526 in Spain. *Resour. Conserv. Recycl.* 175, 105838.  
527 <https://doi.org/10.1016/j.resconrec.2021.105838>
- 528 Biles, W.E., Kleijnen, J.P.C., van Beers, W.C.M., van Nieuwenhuyse, I., 2007. Kriging  
529 metamodeling in constrained simulation optimization: an explorative study, in:  
530 2007 Winter Simulation Conference. IEEE, pp. 355–362.  
531 <https://doi.org/10.1109/WSC.2007.4419623>
- 532 CEN, 2004. Eurocode 2: Design of concrete structures - Part 1-1: General rules and  
533 rules for buildings.

534 Connolly, D., Giannopoulos, A., Forde, M.C., 2013. Numerical modelling of ground  
535 borne vibrations from high speed rail lines on embankments. *Soil Dyn. Earthq.*  
536 *Eng.* 46, 13–19. <https://doi.org/10.1016/j.soildyn.2012.12.003>

537 Cortina Ruiz, E., 2013. La utilización de la vía en placa en líneas de alta velocidad:  
538 aplicación práctica. Universitat Politècnica de Catalunya.

539 Dette, H., Pepelyshev, A., 2010. Generalized Latin Hypercube Design for Computer  
540 Experiments. *Technometrics* 52, 421–429.  
541 <https://doi.org/10.1198/TECH.2010.09157>

542 Eaton, J., Yang, S., Gongora, M., 2017. Ant Colony Optimization for Simulated  
543 Dynamic Multi-Objective Railway Junction Rescheduling. *IEEE Trans. Intell.*  
544 *Transp. Syst.* 18, 2980–2992. <https://doi.org/10.1109/TITS.2017.2665042>

545 Esveld, C., 2001. *Modern Railway Track*, 2nd ed. TU Delft.

546 European Commission, 2020. *EU transport in figures - Statistical Pocketbook 2020*.  
547 <https://doi.org/10.2832/491038>

548 European Commission, 2018. *A Clean Planet for all. A European strategic long-term*  
549 *vision for a prosperous, modern, competitive and climate neutral economy -*  
550 *Communication from the Commission to the European Parliament, the Council,*  
551 *the European and Social Committee and the Committee.*

552 Ferdous, W., Manalo, A., Siddique, R., Mendis, P., Zhuge, Y., Wong, H.S., Lokuge,  
553 W., Aravinthan, T., Schubel, P., 2021. Recycling of landfill wastes (tyres, plastics  
554 and glass) in construction – A review on global waste generation, performance,  
555 application and future opportunities. *Resour. Conserv. Recycl.* 173, 105745.  
556 <https://doi.org/10.1016/j.resconrec.2021.105745>

557 Fernández, A., Fernández-Cardador, A., Cucala, P., Domínguez, M., Gonsalves, T.,  
558 2015. Design of Robust and Energy-Efficient ATO Speed Profiles of Metropolitan

559 Lines Considering Train Load Variations and Delays. *IEEE Trans. Intell. Transp.*  
560 *Syst.* 16, 2061–2071. <https://doi.org/10.1109/TITS.2015.2391831>

561 Frischknecht, R., Rebitzer, G., 2005. Theecoinvent database system: a comprehensive  
562 web-based LCA database. *J. Clean. Prod.* 13, 1337–1343.  
563 <https://doi.org/10.1016/j.jclepro.2005.05.002>

564 García-Segura, T., Penadés-Plà, V., Yepes, V., 2018. Sustainable bridge design by  
565 metamodel-assisted multi-objective optimization and decision-making under  
566 uncertainty. *J. Clean. Prod.* 202, 904–915.  
567 <https://doi.org/10.1016/j.jclepro.2018.08.177>

568 Gautier, P.-E., 2015. Slab track: Review of existing systems and optimization potentials  
569 including very high speed. *Constr. Build. Mater.* 92, 9–15.  
570 <https://doi.org/10.1016/j.conbuildmat.2015.03.102>

571 Ghasemalizadeh, O., Khaleghian, S., Taheri., S., 2016. A review of optimization  
572 techniques in artificial networks. *Int. J. Adv. Res.* 4, 1668–1686.  
573 <https://doi.org/10.21474/IJAR01/1627>

574 Goedkoop, M., Heijungs, R., Huijbregts, M., De Scheryver, A., Struijs, J., van Zelm, R.,  
575 2009. ReCiPe 2008: A life cycle impact assessment method which comprises  
576 harmonised category indicators at the midpoint and the endpoint level.

577 Hall, L., 2003. Simulations and analyses of train-induced ground vibrations in finite  
578 element models. *Soil Dyn. Earthq. Eng.* 23, 403–413.  
579 [https://doi.org/10.1016/S0267-7261\(02\)00209-9](https://doi.org/10.1016/S0267-7261(02)00209-9)

580 Hidalgo Signes, C., Martínez Fernández, P., Garrido De La Torre, M.E., Insa Franco,  
581 R., 2016. Unbound granular materials for sub-ballast layers and their mixing with  
582 rubber particles from scrap tyres. *Civil-Comp Proc.* 110.

583 Jakubek, D., Wagner, C., 2016. Aerodynamic shape optimization of train heads using

584       adjoint-based computational fluid dynamics with different objective functions, in:  
585       Proceedings of the Third International Conference on Railway Technology:  
586       Research, Development and Maintenance. Cagliari.

587   Jin, Q., Thompson, D.J., Lurcock, D.E.J., Toward, M.G.R., Ntotsios, E., 2018. A 2.5D  
588       finite element and boundary element model for the ground vibration from trains in  
589       tunnels and validation using measurement data. *J. Sound Vib.* 422, 373–389.  
590       <https://doi.org/10.1016/j.jsv.2018.02.019>

591   Kaewunruen, S., Sresakoolchai, J., Peng, J., 2020. Life cycle cost, energy and carbon  
592       assessments of Beijing-Shanghai high-speed railway. *Sustainability* 12, 1–18.  
593       <https://doi.org/10.3390/SU12010206>

594   Kirkpatrick, S., Gelatt, C.D., Vecchi, M.P., 1983. Optimization by Simulated  
595       Annealing. *Science* (80-. ). 220, 671–680.  
596       <https://doi.org/10.1126/science.220.4598.671>

597   Kortazar, A., Bueno, G., Hoyos, D., 2021. Dataset for the life cycle assessment of the  
598       high speed rail network in Spain. *Data Br.* 36.  
599       <https://doi.org/10.1016/j.dib.2021.107006>

600   Li, L., Nimbalkar, S., Zhong, R., 2018. Finite element model of ballasted railway with  
601       infinite boundaries considering effects of moving train loads and Rayleigh waves.  
602       *Soil Dyn. Earthq. Eng.* 114, 147–153.  
603       <https://doi.org/10.1016/j.soildyn.2018.06.033>

604   Lichtberger, B., 2011. *Track Compendium*, 2nd ed. DVV Media Group GmbH,  
605       Hamburg.

606   Lophaven, S.N., Nielsen, H.B., Sondergaard, J., 2002. *DACE - A Matlab Kriging*  
607       Toolbox, Version 2.0 [WWW Document]. URL  
608       <http://www.imm.dtu.dk/pubdb/p.php?3213> (accessed 7.5.21).

609 Martínez Fernández, P., Salvador Zuriaga, P., Villalba Sanchís, I., Insa Franco, R.,  
610 2019a. Neural networks for modelling the energy consumption of metro trains.  
611 Proc. Inst. Mech. Eng. Part F J. Rail Rapid Transit 0, 1–12.  
612 <https://doi.org/10.1177/0954409719861595>

613 Martínez Fernández, P., Villalba Sanchís, I., Botello, F., Insa Franco, R., 2013.  
614 Monitoring and analysis of vibration transmission for various track typologies. A  
615 case study. Transp. Res. Part D Transp. Environ. 24, 98–109.

616 Martínez Fernández, P., Villalba Sanchís, I., Yepes, V., Insa Franco, R., 2019b. A  
617 review of modelling and optimisation methods applied to railways energy  
618 consumption. J. Clean. Prod. 222, 153–162.  
619 <https://doi.org/10.1016/j.jclepro.2019.03.037>

620 Matheron, G., 1963. Principles of geostatistics. Econ. Geol. 58, 1246–1266.  
621 <https://doi.org/10.2113/gsecongeo.58.8.1246>

622 Medina, J.R., 2001. Estimation of Incident and Reflected Waves Using Simulated  
623 Annealing. J. Waterw. Port, Coastal, Ocean Eng. 127, 213–221.  
624 [https://doi.org/10.1061/\(ASCE\)0733-950X\(2001\)127:4\(213\)](https://doi.org/10.1061/(ASCE)0733-950X(2001)127:4(213))

625 Michas, G., 2012. Slab Track Systems for High-Speed Railways. Royal Institute of  
626 Technology.

627 Ministerio de Fomento, 1999. Recomendaciones para el proyecto de plataformas  
628 ferroviarias, 1st ed. Centro de Publicaciones Secretaría General Técnica Ministerio  
629 de Fomento, Spain.

630 Mohamad, N., Muthusamy, K., Embong, R., Kusbiantoro, A., Hashim, M.H., 2021.  
631 Environmental impact of cement production and Solutions: A review. Mater.  
632 Today Proc. <https://doi.org/10.1016/j.matpr.2021.02.212>

633 Myers, R.H., Montgomery, D.C., Anderson-Cook, C.M., 2016. Response Surface

634 Methodology: Process and Product Optimization Using Designed Experiments.  
635 John Wiley & Sons.

636 Olsson, A., Sandberg, G., Dahlblom, O., 2003. On Latin hypercube sampling for  
637 structural reliability analysis. *Struct. Saf.* 25, 47–68.  
638 [https://doi.org/10.1016/S0167-4730\(02\)00039-5](https://doi.org/10.1016/S0167-4730(02)00039-5)

639 Penadés-Plà, V., García-Segura, T., Yepes, V., 2020a. Robust Design Optimization for  
640 Low-Cost Concrete Box-Girder Bridge. *Mathematics* 8, 398.  
641 <https://doi.org/10.3390/math8030398>

642 Penadés-Plà, V., García-Segura, T., Yepes, V., 2019. Accelerated optimization method  
643 for low-embodied energy concrete box-girder bridge design. *Eng. Struct.* 179,  
644 556–565. <https://doi.org/10.1016/j.engstruct.2018.11.015>

645 Penadés-Plà, V., Yepes, V., García-Segura, T., 2020b. Robust decision-making design  
646 for sustainable pedestrian concrete bridges. *Eng. Struct.* 209, 109968.  
647 <https://doi.org/10.1016/j.engstruct.2019.109968>

648 Pita, A.L., Teixeira, P.F., Robuste, F., 2004. High speed and track deterioration: The  
649 role of vertical stiffness of the track. *Proc. Inst. Mech. Eng. Part F J. Rail Rapid*  
650 *Transit* 218, 31–40. <https://doi.org/10.1243/095440904322804411>

651 Pons, J.J., Penadés-Plà, V., Yepes, V., Martí, J. V., 2018. Life cycle assessment of  
652 earth-retaining walls: An environmental comparison. *J. Clean. Prod.* 192, 411–420.  
653 <https://doi.org/10.1016/j.jclepro.2018.04.268>

654 Pons, J.J., Villalba Sanchis, I., Insa Franco, R., Yepes, V., 2020. Life cycle assessment  
655 of a railway tracks substructures: Comparison of ballast and ballastless rail tracks.  
656 *Environ. Impact Assess. Rev.* 85, 106444.  
657 <https://doi.org/10.1016/j.eiar.2020.106444>

658 Sayeed, M.A., Shahin, M.A., 2016. Three-dimensional numerical modelling of ballasted

659 railway track foundations for high-speed trains with special reference to critical  
660 speed. *Transp. Geotech.* 6, 55–65. <https://doi.org/10.1016/j.trgeo.2016.01.003>

661 Selig, E.T., Waters, J.M., 1994. *Track Geotechnology and Substructure Management*.  
662 Thomas Telford Publishing. <https://doi.org/10.1680/tgasm.20139>

663 Simpson, T.W., Mauery, T.M., Korte, J.J., Mistree, F., 2001. Kriging Models for Global  
664 Approximation in Simulation-Based Multidisciplinary Design Optimization. *AIAA*  
665 *J.* 39, 2233–2241. <https://doi.org/10.2514/2.1234>

666 Tuchschnid, M., Knörr, W., Schach, A., Mottschall, M., 2011. Carbon Footprint and  
667 environmental impact of railway infrastructure.

668 UIC, 2008. UIC Leaflet 719R - Earthworks and track bed for railway lines.

669 Villalba Sanchis, I., Insa Franco, R., Martínez Fernández, P., Salvador Zuriaga, P.,  
670 2021. Experimental and numerical investigations of dual gauge railway track  
671 behaviour. *Constr. Build. Mater.* 299, 123943.  
672 <https://doi.org/10.1016/j.conbuildmat.2021.123943>

673 Wang, B., Yan, L., Fu, Q., Kasal, B., 2021. A Comprehensive Review on Recycled  
674 Aggregate and Recycled Aggregate Concrete. *Resour. Conserv. Recycl.* 171,  
675 105565. <https://doi.org/10.1016/j.resconrec.2021.105565>

676 Woods, D.C., Lewis, S.M., 2017. Design of Experiments for Screening, in: *Handbook*  
677 *of Uncertainty Quantification*. Springer International Publishing, Cham, pp. 1143–  
678 1185. [https://doi.org/10.1007/978-3-319-12385-1\\_33](https://doi.org/10.1007/978-3-319-12385-1_33)

679 Ye, Y., Sun, Y., 2021. Reducing wheel wear from the perspective of rail track layout  
680 optimization. *Proc. Inst. Mech. Eng. Part K J. Multi-body Dyn.* 235, 217–234.  
681 <https://doi.org/10.1177/1464419320956831>

682 Ye, Y., Sun, Y., Dongfang, S., Shi, D., Hecht, M., 2021. Optimizing wheel profiles and  
683 suspensions for railway vehicles operating on specific lines to reduce wheel wear:



684 a case study. *Multibody Syst. Dyn.* 51, 91–122. <https://doi.org/10.1007/s11044->  
685 020-09722-4

686 Zhao, Y., Li, X., Lv, Q., Jiao, H., Xiao, X., Jin, X., 2017. Measuring, modelling and  
687 optimising an embedded rail track. *Appl. Acoust.* 116, 70–81.  
688 <https://doi.org/10.1016/j.apacoust.2016.07.021>  
689

690 **Table 1.** Optimal values of slab cross-section from each kriging surface and constraints  
 691 checking.

| Kriging surface | Slab thickness (cm) | $f_{ck}$ (MPa) | $f_{tck}$ (MPa) | Rail displacement (mm) | Rail stress (Von Misses) (MPa) | Track vertical stiffness (kN/mm) | Slab max. stress (MPa)     |
|-----------------|---------------------|----------------|-----------------|------------------------|--------------------------------|----------------------------------|----------------------------|
| 1               | 29                  | 40             | 2.46            | 2.872                  | 68.3                           | 81.82                            | 0.464                      |
| 2               | 26                  | 45             | 2.66            | 2.879                  | 68.3                           | 81.63                            | 0.497                      |
| 3               | 25                  | 45             | 2.66            | 2.882                  | 68.4                           | 81.54                            | 0.509                      |
| 4               | 27                  | 45             | 2.66            | 2.877                  | 68.3                           | 81.68                            | 0.484                      |
| 5               | 30                  | 40             | 2.46            | 2.869                  | 68.3                           | 81.91                            | 0.453                      |
| 6               | 24                  | 45             | 2.66            | 2.886                  | 68.4                           | 81.43                            | 0.523                      |
| 7               | 34                  | 35             | 2.25            | 2.861                  | 68.2                           | 82.14                            | 0.424                      |
| 8               | 32                  | 35             | 2.25            | 2.866                  | 68.2                           | 82.00                            | 0.440                      |
| 9               | 24                  | 45             | 2.66            | 2.886                  | 68.4                           | 81.43                            | 0.523                      |
| Constraint      | —                   | —              | —               | $\leq 3$               | $\leq 137.5$                   | [75, 85]                         | $\leq \frac{f_{tck}}{4.1}$ |
| Checks?         | —                   | —              | —               | Yes                    | Yes                            | Yes                              | Yes                        |

692

693 **Table 2.** Optimal values of slab cross-section from each kriging surface and comparison  
 694 of cost values.

| Kriging surface | Slab thickness (cm) | $f_{ck}$ (MPa) | $f_{tck}$ (MPa) | Predicted cost (€/km) | Real cost (€/km) | Cost variability | Cost reduction |
|-----------------|---------------------|----------------|-----------------|-----------------------|------------------|------------------|----------------|
| 1               | 29                  | 40             | 2.46            | 59,530.98             | 61,797.84        | 3.67%            | 3.33%          |
| 2               | 26                  | 45             | 2.66            | 54,445.45             | 57,378.88        | 5.11%            | 10.25%         |
| 3               | 25                  | 45             | 2.66            | 52,654.37             | 55,172.00        | 4.56%            | 13.70%         |
| 4               | 27                  | 45             | 2.66            | 55,097.51             | 59,585.76        | 7.53%            | 6.79%          |
| 5               | 30                  | 40             | 2.46            | 64,342.17             | 63,928.80        | 0.64%            | 0.00%          |
| 6               | 24                  | 45             | 2.66            | 56,823.80             | 52,965.12        | 6.79%            | 17.15%         |
| 7               | 34                  | 35             | 2.25            | 62,036.69             | 66,609.40        | 6.86%            | -4.19%         |
| 8               | 32                  | 35             | 2.25            | 62,691.51             | 62,691.20        | 0.00%            | 1.94%          |
| <b>9</b>        | <b>24</b>           | <b>45</b>      | <b>2.66</b>     | <b>50,880.00</b>      | <b>52,965.12</b> | <b>3.94%</b>     | <b>17.15%</b>  |
| Mean            | —                   | —              | —               | 57,611.39             | 59,232.68        | 4.35%            | 7.35%          |

695

696

697 **Table 3.** Comparison of costs and impacts between the original cross-section and the  
 698 optimised one.

| Parameter                                   | Original section | Optimised section | Reduction |
|---|------------------|-------------------|-----------|
| Thickness (cm)                              | 30               | 24                | —         |
| $f_{ck}$ (MPa)                              | 40               | 45                | —         |
| $f_{tck}$ (MPa)                             | 2.46             | 2.66              | —         |
| Real cost (€/km)                            | 63,928.80        | 52,965.12         | 17.15%    |
| Impact on resources (\$)                    | 62,425.93        | 52,894.84         | 15.27%    |
| Impact on ecosystems<br>(species.year)      | 0.00328          | 0.00205           | 37.50%    |
| Impact on human health<br>(DALY)            | 0.47278          | 0.38938           | 17.64%    |
| Impact on safety (hours of<br>average risk) | 480,760.10       | 386,774.24        | 19.55%    |

699